Astron. Astrophys. 266, 6–14 (1992)

ASTRONOMY AND ASTROPHYSICS

The system of arcs in the cluster of galaxies Abell 2218: photometry, spectroscopy and geometry*

R. Pelló[1], J.F. Le Borgne[2], B. Sanahuja[1], G. Mathez[2] and B. Fort[2]

[1] Departament d'Astronomia i Meteorologia, Universitat de Barcelona, and Laboratori d'Astrofísica del IEC, Diagonal 647, E-08028 Barcelona, Spain

[2] Observatoire Midi-Pyrénées, 14 avenue Edouard Belin, F-31400 Toulouse, France

Received April 8, accepted August 28, 1992

Abstract. We analyse in this paper new photometric and spectroscopic data on the system of arcs in the center of the rich cluster of galaxies A2218. 32 arc(let)s have been identified in the field, with colours compatible with high redshift galaxies ($z > 0.6$) in most cases. From the spectroscopic survey, it is found that A2218 exhibits a complex dynamical structure, with a possible double system formed by the central cD and galaxies #244 and #259. This point is also confirmed by the arc(let)s configuration. For the first time, we give spectroscopic results for three arc structures. We discuss the identification of 2 arcs as high redshift objects (z =1.034 and z =0.702, respectively), result that allows the confirmation of the gravitational lens hypothesis. The presence of a complete ring around a bright galaxy close to the center of the cluster is also discussed. We consider the implications on the mass distribution inside the cluster, as derived from these results. The whole spectroscopic, photometric and geometric information required for the construction of a model for the cluster potential is given.

Key words: clusters of galaxies: Abell 2218 – redshifts of galaxies – gravitational lensing: Arcs.

1. Introduction

Abell 2218 is classified in the Abell's catalogue (Abell et al. 1989) as a cluster of richness class 4 and a redshift of 0.171. This redshift was measured by Kristian et al. (1978) from the spectrum of the main galaxy of the cluster. A2218 belongs to the Butcher and Oemler's photometric sample (Butcher et al. 1983; Butcher & Oemler 1984), in which it is one of the richest and most concentrated clusters, with a concentration parameter C=0.59. It is mainly known to exhibit a Sunyaev-Zeldovich effect (Birkinshaw et al. 1981; Birkinshaw & Gull 1984; Partridge et al. 1987; Klein et al. 1991). In addition, A2218 is one of the closest clusters in which arcs and arclets have been found up to now. A first description and photometry of such structures have been published by Pelló et al. (1988) (hereafter referred as Paper I). Recently, Le Borgne et al. (1992) have published a more detailed photometric and spectroscopic survey on this cluster, which will be used here as a database for the objects in this field (it is referred hereafter as Paper II). From this spectroscopic survey, it results a mean redshift of 0.1756 and a velocity dispersion of 1370 km s^{-1} for the cluster.

In the present paper, we report new photometric and spectroscopic observations of arcs and arclets found near the center of the cluster. The basic description of the observational runs can be found in Paper II, but the information is summarized and completed in Sect. 2. In Sect. 3 we present new data on the main arc structures and we give a photometric catalogue of the arclets detected in the central region. A general discussion of the results is available in Sect. 4. Throughout this paper, we assume H_o=50 km sec^{-1} Mpc^{-1} and q_o=0.

2. Observations

The photometric observations were mainly performed at the 3.5m telescope of the Centro Astronomico Hispano Alemán de Calar Alto (Almería, Spain), and the spectroscopic ones at the 4.2m William Herschel Telescope at La Palma (Canary Islands, Spain). The filters used were a Johnson B and Thuan-Gunn g, r, i and z. Spectra of galaxies and arcs were obtained with the Faint Objet Spectrograph of the WHT set on its red channel (Allington-Smith et al. 1989). In this paper we present new spectroscopic data concerning three arcs. A detailed description of the photometric and spectroscopic observations, calibrations and data reduction can be found in Paper II, together with several general results concerning this cluster, . In particular, Table 2 and Table 3 in Paper II give, respectively, the Bgriz photometry and the spectroscopic data for each galaxy. The identification numbers used hereafter come from these tables.

Several U frames were also obtained at the Cassegrain focus of the 2 m telescope Bernard Lyot (Observatoire du Pic du Midi, France) in July 1991, using a coated Thomson 1024 × 1024 CCD which was under test during the run. These images concern only a small field of 1′20″ square, in the close neighbourhood of the

Send offprint requests to: R. Pelló

* Based on observations made with the 3.5m telescope of the Centro Astronómico Hispano-Alemán de Calar Alto, with the William Herschel Telescope operated on the island of La Palma by the Royal Greenwich Observatory in the spanish Observatorio del Roque de los Muchachos of the Instituto de Astrofísica de Canarias and the Télescope Bernard Lyot at Pic du Midi Observatory.

Table 1. Photometric UB catalogue for the objects near the central galaxy.

#	μ_U	B	U	U-B	B-r
305	23.20	21.07	20.97	-1.10	0.48
320	23.82	20.99	21.38	-0.58	1.78
322	23.53	21.88	21.65	-0.59	0.62
341	22.94	19.96	20.75	-0.02	2.00
346	22.45	20.66	20.65	-0.26	0.65
348	23.51	21.51	22.22	0.12	1.70
360	23.68	20.64	21.62	-0.19	1.76
373	23.35	20.24	21.82	0.58	1.81
384	25.49	22.35	22.67	0.24	0.75
385	23.56	20.14	21.28	0.25	1.60
391	23.59	19.09	21.05	-0.35	1.79
395	22.13	20.06	19.83	-0.59	0.89
421	23.22	21.23	21.06	-0.72	1.74
422	24.20	21.29	21.27	-0.59	1.83
430	23.29	20.48	21.32	0.07	1.94
436	23.79	20.65	21.09	-0.15	1.73
446	23.41	20.78	21.56	-0.07	1.90
448	23.74	21.88	21.63	-0.62	1.73
467	23.33	22.07	21.17	-1.54	0.98
482	22.92	19.83	21.12	0.23	1.82

central cD galaxy. The pixel size was 0.31″and the mean quantum efficiency in the U band was only 3% . Due to the low efficiency of the UV sensitive coating, we needed 13 exposures of 3600 seconds to attain a surface brightness of about 25.5 mag arcsec^{-2} in U at 1σ of the sky noise. The quality of these images is poor compared to those obtained previously (paper II), but they are of great interest because they allow to complete the study of the spectral energy distribution of the objects around the cD galaxy.

A complementary catalogue with the UB photometry is presented in Table 1. In this case, instead of the automatic procedure, we applied an interactive fit of the isophotal contours to obtain the U mag inside the isophote μ_U=26 mag arcsec^{-2}. The U-B colour has been calculated inside the limiting U isophote fitted by hand. Columns in Table 1 give, for each object and from left to right: identification number, central surface brightness in U, B mag (limiting isophote 27 mag arcsec^{-2}), U mag (limiting isophote 26 mag arcsec^{-2}), U-B and B-r. B and B-r have been taken from Paper II. We estimate that the photometric accuracy attained here for the U filter is worse than that given in Paper II for the other magnitudes: the typical error is 0.3 mag for objects up to U=21-22.

3. Photometry and spectroscopy of the arcs

The brightest arcs in A2218 have already been described in Paper I. The new CCD frames obtained since 1988, and especially those obtained in 1991, show a large quantity of fainter arclets that appear as fine and unresolved elongated structures. Furthermore, several details can be seen in arcs H and L. The identification of the different objects in the present paper follows the numbering given in Paper II. The new identifications for the main arc structures presented in Paper I are: #384 (A), #444 (A'), #424 (B), #359 (H), #289 (L) and #730 (L').

The photometric characteristics of the different arc structures are given in Table 2. We have considered as arclet candidates

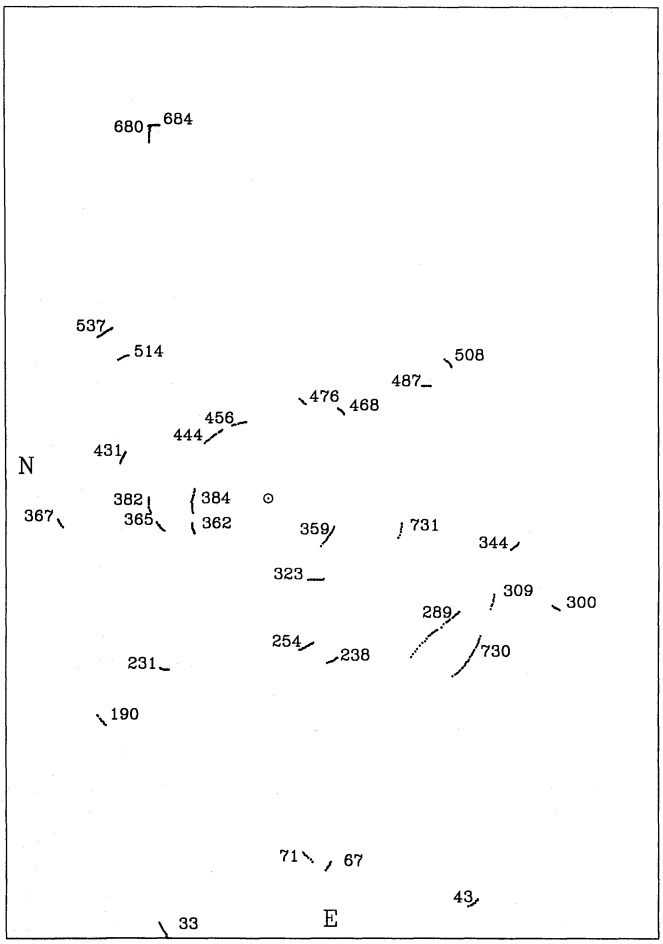

Fig. 1. Identification chart of the arcs and arclets found in the field of A2218. The size of the field and the identification numbers are the same as in Figs. 1 to 3 of Paper II.

all the objects showing a ratio between the total length and the FWMH above 3. This definition includes 32 objects in the field. The information given in Table 2 is, from left to right: identification number, x and y coordinates in arc seconds with respect to the central galaxy, increasing southward and westward respectively, r magnitude, B-r, g-r, r-z, total length in arc seconds, orientation angles θ_1 and θ_2 and photometric redshift (when available, the spectroscopic redshift is given in parenthesis). θ_1 is the orientation angle of the arclet with respect to the N direction, increasing eastward ($0° \leq \theta_1 \leq 180°$). The orientation with respect to the central galaxy, θ_2, is defined as the angle between the radial position vector of the arclet and the normal to the arclet, positive anticlockwise ($-90° \leq \theta_2 \leq 90°$). A value of $\theta_2 \approx 0°$ identifies an object almost perpendicular to its position vector. The magnitudes and colours given in this table have been calculated inside the limiting isophotal magnitude $\mu_r = 26$ mag arcsec^{-2} fitted by hand. The difference between the values given here and those presented in Paper II for the magnitudes and colours are due to the fact that objects here have not been forced to fit an elliptical shape. When calculating magnitudes and colours in B and r, we give the values obtained by averaging the results coming from long and composite exposures. The colours are found to be the same, within errors, when different limiting isophotes are used, except in a few cases. Objects #289 and #359

Table 2. Some geometric and photometric characteristics of the arcs and related objects.

Objects	x (″)	y (″)	r	B-r	g-r	r-z	L (″)	θ_1 (°)	θ_2 (°)	photometric redshift
33	-30.96	-125.69	22.22	2.01	–	0.62	4.8	115	-51	0.4-1.4
43	59.87	-117.88	22.59	1.31	–	0.60	2.5	37	10	0.0-2.5
67	17.22	-107.46	24.03	1.40	1.45	0.15	3.2	61	52	2.0-3.0
71	12.56	-106.22	23.81	1.61	1.19	0.81	3.8	132	-54	0.5-1.6/2.0-2.5
190	-48.90	-64.71	23.04	1.71	1.10	0.46	3.2	129	-14	0.1-0.7/2.0-2.6
231	-30.52	-49.85	22.50	1.31	1.23	0.35	2.6	163	14	0.2-0.7/2.0-2.6
238	18.68	-47.44	22.68	1.26	1.21	0.23	4.2	25	4	2.0-3.0
254	11.07	-43.48	23.03	1.80	1.09	0.28	4.9	28	14	0.2-0.7/2.2-3.0
289	53.78	-35.02	21.67	0.75	0.09	0.95	6.7	37	-20	0.8-2.4 (1.034)
300	84.62	-32.10	24.37	1.17	0.44	0.83	2.2	144	75	0.8-2.5
309	66.24	-28.65	24.98	0.72	-0.29	2.08	4.1	60	5	1.4-2.0
323	13.86	-23.75	21.94	1.60	-0.15	0.56	4.0	4	-26	1.4-1.6/2.0-2.6
344	71.42	-14.53	23.30	1.20	0.12	0.20	3.0	41	-38	1.8-3.0
359	17.94	-10.53	21.40	2.89	1.30	0.70	5.8	56	-4	0.5-0.7 (0.702)
362	-21.88	-8.80	23.43	1.19	0.22	0.26	2.9	105	-7	0.0-0.3/1.8-3.0
365	-31.74	-7.75	24.23	2.39	0.23	0.24	3.4	126	21	2.4-3.0
367	-61.16	-6.61	23.47	1.21	0.34	–	3.0	121	24	0.0-0.3/0.7-3.3
382	-34.84	-1.81	24.10	0.39	-0.35	0.49	5.1	90	-3	1.4-2.6
384	-22.05	-1.33	21.68	0.75	0.24	-0.02	7.1	84	-9	0.0-0.3/2.6-3.5
431	-42.44	12.58	23.26	0.79	0.24	0.99:	5.0	66	-8	0.8-2.4
444	-17.25	17.14	23.39	0.35	0.19	0.19	6.3	37	-6	1.8-3.0
456	-7.97	22.02	22.88	1.64	0.90	0.35	4.3	13	-7	0.1-0.7/1.4-2.6
468	21.44	25.78	23.62	0.81	-0.01	0.23	2.3	139	-1	1.8-3.0
476	9.83	28.37	24.25	0.53	0.00	0.73	2.5	135	-25	1.2-2.6
487	46.54	32.96	23.03	1.02	-0.05	0.37	2.1	0	55	2.2 -2.6
508	52.18	40.53	24.87	0.57	0.06	-0.22	2.7	139	12	2.4-3.3
514	-41.53	41.54	24.54	1.19	1.37	1.52	2.6	17	-29	0.8-1.5/2.1-2.2
537	-47.43	48.89	22.38	1.68	1.55	0.83	4.9	28	-16	0.5-1.4/2.1-2.5
680	-34.47	106.88	22.18	1.63	0.42	0.71	5.6	87	69	1.2-1.6/2.0-2.6
684	-32.90	109.24	23.81	1.00	1.42	0.87	2.6	169	-11	0.5-1.4/2.2-2.5
730	54.28	-41.97	21.93	1.43	0.22	-0.39	22.0	-	-	2.9-3.3
731	38.96	-9.36	23.70	0.99	0.17	-0.09	3.3	67	9	2.3-3.1

seem to show some evidence for a colour gradient in B-r. Besides, the small differences found for several very faint objects inside the cD halo, as #362, are probably due to a deficient correction for the contamination by this halo.

We present in Fig. 1 the identification chart for all the arcs and arclets found in this field, where the lines define the length of the objects up to about 1σ of the sky noise in r. The center of the cD galaxy is also indicated. About two thirds of the arclets are nearly perpendicular to their corresponding position vector with respect to the central cD or, at least, they are perpendicular to a position vector that crosses the cD halo.

In order to test the reliability of our photometry when trying to obtain some information about the energy distribution in the spectra, we show that it is possible to fit the observed (or synthetic) spectra by the observed photometric fluxes in the different filter bands, from U to z. The result in the case of an elliptical galaxy is plotted in Fig. 2, where the thick line is the averaged spectrum obtained from 20 bright E/S0 galaxies belonging to the cluster. There is a well defined colour-magnitude relation for the E/S0 cluster galaxies, which dominate the cluster population (Table 3). The slopes obtained for the colour-magnitude relation in the different filter pairs are roughly in good agreement with the prediction given by Visvanathan & Sandage (1977). The energy inside the filters has been normalized in order to fit the arbitrary flux of the spectrum in the r band. Vertical error bars indicate the photometrical uncertainties, and the horizontal bars correspond to the filter effective bandpasses. There is a good agreement between the observed spectra of the bright E/S0 type galaxies at the redshift of the cluster, and a synthetic spectrum obtained with Bruzual's evolutionary code for the same type of galaxy (Bruzual & Charlot 1991). The synthetic spectrum corresponds to a galaxy that evolves after a 1Gyr burst at the epoch of its formation (z = 4.45, so 16 Gyr ago), as it appears at a redshift of 0.175 (therefore, when it is about 13 Gyr old).

We have calculated the photometric redshifts of the objects in Table 2 using the colour-redshift diagrams obtained from the Bruzual code for the spectrophotometric evolution of galaxies. Five spectromorphological types of galaxies, ranging from E to Im, have been considered; they define, at a fixed redshift, the upper and lower expected values for each colour index. The present age of all these galaxies was assumed to be 16 Gyrs, so the redshift of formation is about 4.45. These predictions have been performed taking into account the "real" filter transmissions and the quantum efficiencies of the different CCDs used. The photometric redshift for each object has been obtained by using simultaneously the predictions for the colours B-r, g-r and r-z. B-r

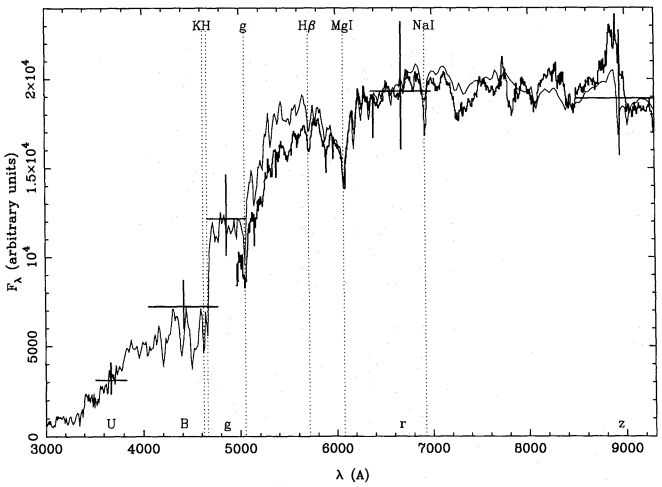

Fig. 2. Comparison between the spectra of the E/S0 type galaxies of the cluster (thick line) and a synthetic E galaxy (thin line), obtained with the Bruzual evolutionary code, at the same redshift. All fluxes are given in arbitrary units. The equivalent flux levels in the different filters are also plotted (see comments in Sect. 3).

Table 3. Slopes of the colour-magnitude relation for the different colour indices and mean values for a r=20 E/S0 galaxy in A2218

colour index	value	slope	limiting isophote and reference filter mag arcsec^{-2}
B-g	0.66	-0.041	g= 27
g-r	0.89	-0.017	r= 26
B-r	1.65	-0.048	r= 26
r-z	0.51	-0.006	r= 26
i-z	0.64	0.042	i= 25

and g-r are useful colours to identify the intermediate from the low and high redshift objects. The index r-z discriminates between objects of redshift higher or lower than 0.5. The "permitted" redshift range for a given object was calculated independently in each colour, and the intersection of these ranges gave the final redshift range for the object. To illustrate the situation for the different objects, Fig. 3 shows a comparison of the colour indices found for all the arcs and arclets with the predicted evolution of the different galaxy types in the diagrams (B-r)/(r-z) and (g-r)/(r-z). Note that the only arc for which a determination of U was possible is #384. We have plotted the positions of all the galaxies identified as cluster members by their spectra. The colours found for these galaxies are in good agreement with the values predicted for E/S0 galaxies at z=0.175, the redshift of the cluster.

When considering the photometric redshifts obtained for the arclet candidates, it appears that only 7 of them are compatible with the redshift of the cluster and, even in this case, these objects are ambiguous because they are also compatible with higher redshift values. When the redshift of a given object is well determined (because we have a good quality spectrum), it is found to be in good agreement with the photometric determination. There are several arclets in the range $-0.2 < (r-z) < 0.5$ whith colours hardly compatible with the continuous evolutionary models. The fit of these objects is improved using single burst models, 0.1 to 1 Gyrs old, at different redshifts ($0.5 < z < 3.5$). For almost all the colors considered here, the theoretical predictions for the photometric redshift give a second set of possible solutions at high redshift ($2.0 < z < 3.5$), which are in general compatible with the low redshift solutions. If we consider that the high redshift solutions are less probable because of the dimming factor in luminosity, then we find that 68% of the population of arclets is compatible with a redshift ranging from 0.6 to 1.6. Nevertheless, 9 arc(let)s in the field (about 29%) show colours only compatible with high redshift solutions ($z > 1.8$), if we are dealing with "standard" objects. The colour-redshift relation has already been used by one of us (Fort 1991) to estimate the distance of the Tyson population. In that case, the model used (Rocca-Volmerange & Guiderdoni 1988) provided the (B-R) and (R-I) colours up to a redshift of 1.7. In the present paper, we have used the Bruzual predictions, taking into account the real filter transmissions, up to a redshift of 3.5. As the galaxy types considered here are "standard", the results are not strongly dependent on the code used (Bruzual or others). The predictions given by the Bruzual's and Rocca-Volmerange & Guiderdoni's codes are very similar when the filters and the redshift range considered are the same.

We have obtained the spectra of 3 of these arcs, labelled #384, #359 and #289. Each one of these objects belongs to a different "structure". We present here the properties of all them: the systems around the central cD galaxy and the secondary system around galaxies #244 and #259.

3.1. The system around the central cD galaxy

The region concerned is shown in detail in Fig. 4. The most remarkable objects in the southern region are #359, #323 (which overlaps the galaxy #319), and the complete ring around the galaxy #373 (see Sect. 3.3). We suggested in Paper I that the arc #359 could extend across galaxy #373. On the new frames, the extension beyond galaxy #373 appears as a faint circular objet, #389, suggesting that it is not a part of the arc #359 but an independent object. The northern region is populated by a number of very faint, elongated and curved objects which design arc-pattern structures around the cD galaxy. Sometimes they appear as brightness enhancements of a unique faint arc structure, as in the case of objects #362 and #384, or #444 and #456. These arclets show a variety of colours, even inside the same arc structure. But all of them are hardly compatible with the redshift of the cluster.

The spectroscopic information about the southern objects comes from 4 exposures of 3600 sec each, taken with a long slit aligned on #389, #373 and #359. Figure 5 shows their spectra (in arbitrary flux units), as they appear after a 2-dimensional composition, followed by a sky subtraction and a standard calibration. The spectrum of arc #359 is the spectrum of a E/Sa galaxy at a redshift of 0.702: it does not show emission lines (except, maybe, a faint [OII] at 3727Å), but it is possible to identify several absorption features, such as the H and K lines, the CN bands and the discontinuity at 4000Å . The shape of the continuum corresponds to a Sa galaxy in the red end, while in the blue end it is better fitted by an E type spectrum. The spectrum of the galaxy #389 has been obtained by subtracting to the original one a spectrum of the galaxy #373, normalized in order to conserve the energy inside several strong absorption lines. Though it is very noisy because of the contamination due to galaxy #373, the whole shape of the spectrum of #389 suggests that it is a dwarf galaxy member of the cluster.

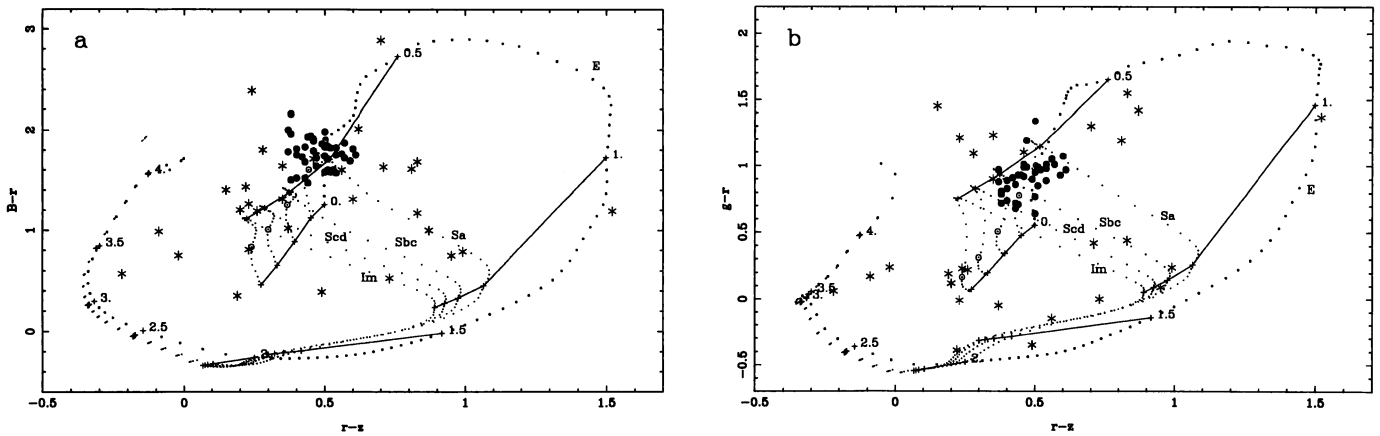

Fig. 3. Examples of colour-colour diagrams used to estimate the colour redshift of the arclet candidates. Evolution curves for different galaxy types are plotted as series of small dots. The isochrones corresponding to z=0 to 4 are represented by thick lines and the expected values for the cluster galaxies (z=0.175) are identified by dotted circles. The data for the arclets are plotted with a * and full dots correspond to galaxies identified as cluster members by their spectra.

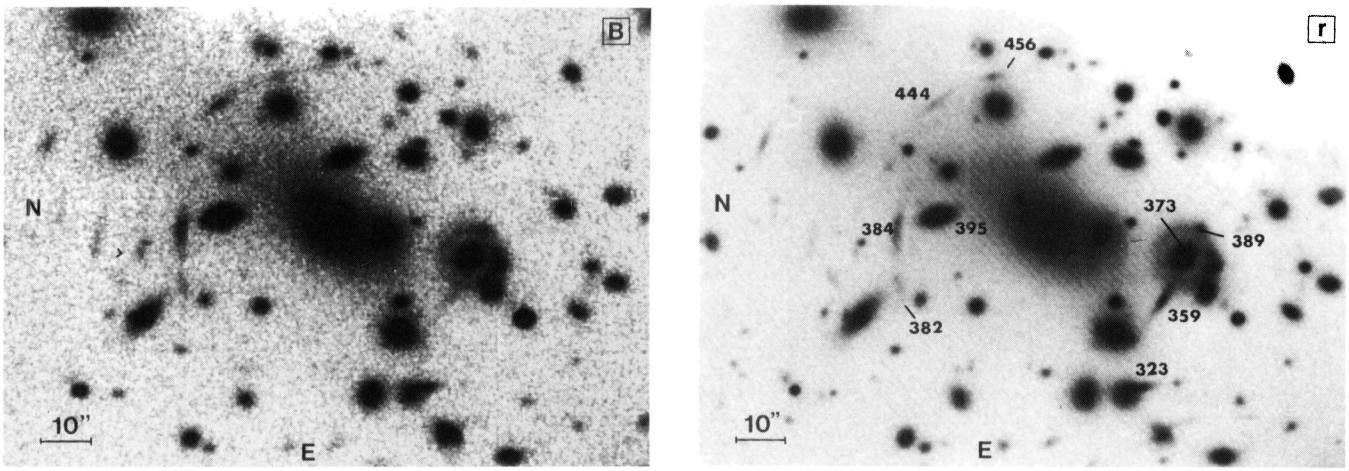

Fig. 4. A detail of the central region in B (left side) and r (right side). The complete ring around the galaxy #373 is clearly visible.

The only arc structure in the northern region for which a useful spectrum has been obtained is #384, the brightest one. This spectrum is the result of a multi-slit observing procedure, in which we tried to obtain simultaneously the spectra of several faint objects. We took 6 exposures of 3600 sec each, using 2 different configurations for the slit. The spectrum of object #384 (shown in Fig. 6) is more puzzling than the other arc spectra presented here: no obvious strong features, neither in absorption nor in emission, can be seen. Taking into account all the colours, from U-B to r-z, it results that this object is only compatible either with a "standard" low redshift galaxy $0.0 < z < 0.3$, or with an extremely high redshift galaxy $2.6 < z < 3.6$. The lowest value for the redshift range at 0.3 is imposed by the g-r, and the cut at 2.6 for the high redshift value is given by the U-B. As it is shown in Fig. 6, the main constraint for the redshift is the existence of a break somewhere between the filters B and U. It may be interpreted either as the 4000Å break with a redshift of about 0.1 or as the discontinuity at 940Å with a high redshift of about 3.6. Nevertheless, the probability of having such a high redshift galaxy without any emission line in the spectrum is very low. Note that Lyα is expected to be found in the spectral range covered by our spectrum. We may tentatively suggest a redshift of 0.09, if we interpret the slight depression around 5600Å as Mgb at 5177Å, and if we accept that the flux in z is slightly lower than predicted in the models. There is another foreground galaxy, #395, very close to this object, with a redshift of 0.103, which shows emission lines in its spectrum. In any case, the spectrum of object #384 does not show any strong absorption or emission line, as it should be expected for a such low redshift object, and it is not compatible with the redshift of the cluster. Besides of this, the object is curved towards the cD, and its shape is actually strange for a foreground object. Altogether, no firm conclusions can be drawn from the material in our hands about the redshift of this object. More data are needed in the blue and the infrared parts of the spectrum.

3.2. The secondary system around galaxies #244 and #259

A detail of the region around galaxies #244 and #259 appears in Fig. 7, where it is possible to see the only giant and almost continuous arc structures detected in this cluster: the objects

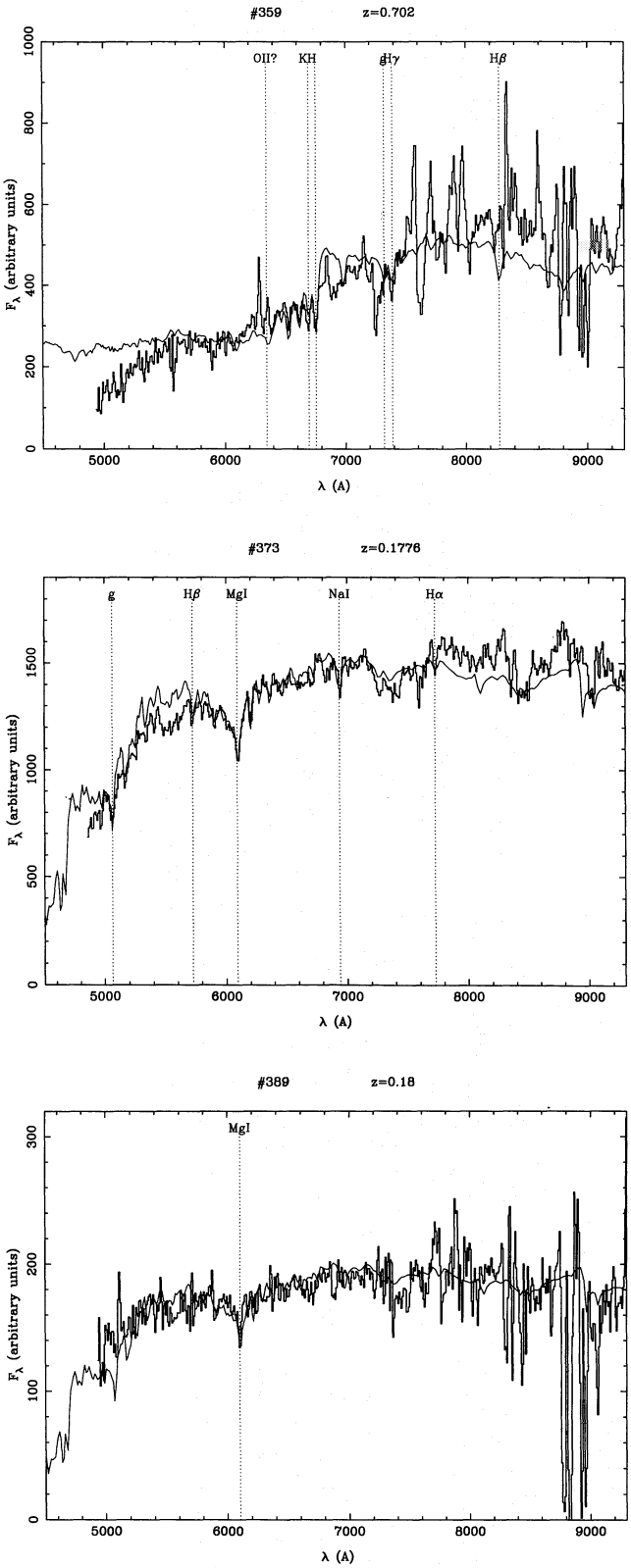

Fig. 5. Spectra of objects #359, #373 and #389

#289 and #730. The former is a rather straight structure, which extends across the halo of the bright galaxies from SW to NE. There is an enhancement in the surface brightness on the SW

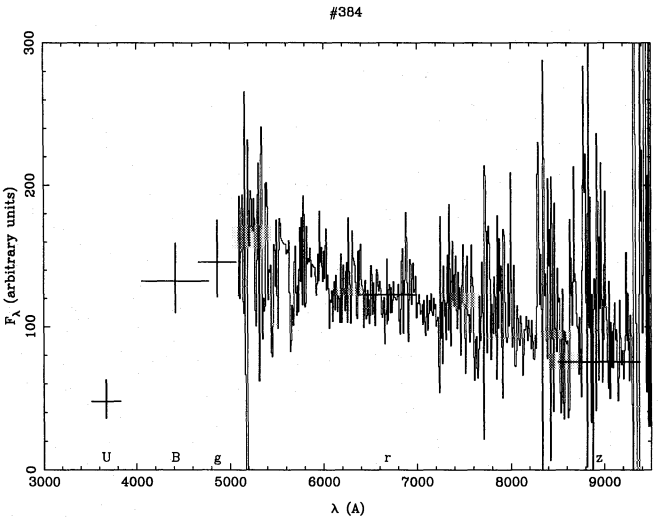

Fig. 6. Spectrum of the object #384

region of this object, where the maximum in μ_r is 22.8 mag arcsec^{-2}. The photometry presented here refers to this bright and straight region, about 7″ of length (28 h_{50}^{-1} *kpc* at the redshift of the cluster), which is not contaminated by the halo. An intensity peak appears in r whereas in B the surface brightness is constant. The object #730 is a very faint and almost circular arc, with a surface brigthness of 23.4 mag arcsec^{-2} in r. Its curvature radius is 33″ (133 h_{50}^{-1} *kpc*) and the curvature center is located 30″ southward and 28″ eastward from the cD galaxy (between the cD and galaxies #244 and #259).

Figure 8 displays the spectrum of the object #289, obtained from 2 exposures of 3600 sec with a long slit aligned on the bright part of the structure. This spectrum shows an emission line at 7581Å which gives a redshift of 1.034, if we identify it as [OII] 3727Å. This identification is consistent with the shape of the continuum: it is flat between 5000 and 7700 Å, and its level increases in the sky-free spectral intervals after 8200 Å. The ratio between the flux levels after and before 8200 Å is about 1.5, which is compatible with a 4000 Å discontinuity at z = 1.034. The insertion in the left-hand side of the figure shows the position of this strong emission line on one of the two 2D sky-cleaned spectra of the object. The emission line is equally bright in both 2D spectra. In fact, it is possible to see this emission line all along the bright part of the structure before any image handling, and it fades when passing to the fainter part of the arc. Nevertheless, this effect can be due to a lack of contrast between the spectrum of the arc and that of the halo of galaxies #244 and #259, which dominates this region in r. In addition, the slit was not perfectly aligned with the faintest part of the structure because it is slightly curved. Though there is no spectrum available for the object #730, the colours given above allow a photometric determination of the redshift which ranges between 2.9 and 3.3.

3.3. The ring around galaxy #373

Since the first B images taken in 1988, it did seem evident that an almost complete ring exists around the galaxy #373 (Fort 1990; Pelló 1990). The presence of such a structure has been confirmed by the high resolution Brz images taken in the run of August 1991. The ring appears as a separate structure with

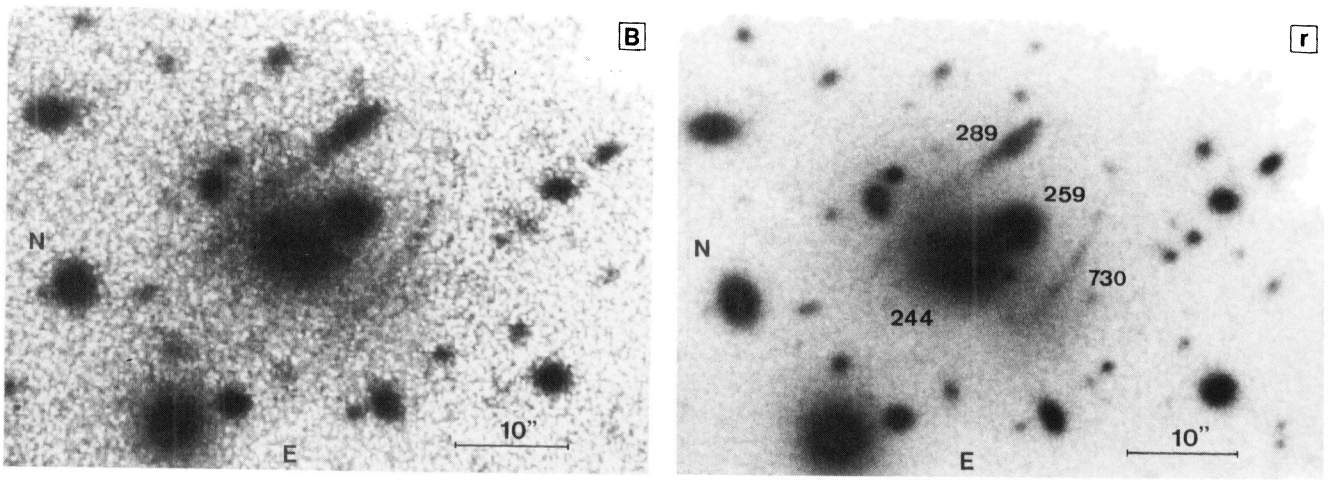

Fig. 7. A detail of the region around galaxies 259 and #244 in B (left side) and r (right side), where 2 giant arcs can be seen.

respect to the galaxy, even without any special image handling, such as a B-R composition of the frames. The formation of a complete ring around a galaxy (an "Einstein ring") is one of the oldest predictions of the gravitational lense theory (Zwicky 1937, among others). Two cases of radio rings have been reported until now: MG 1131+045 (Hewitt et al. 1988) and MG1654+134 (Langston et al. 1989). The possibility of creating an optical ring, well separated with respect to the lens galaxy, as it is observed in the present case, was discussed in a recent paper by Kochanek & Blandford (1991). Such a situation is expected to happen very often when the lens galaxy lies inside a rich cluster, because in this case the cluster mass may contribute to the magnification. It is possible to describe the geometry of this ring by an elliptical fit of the inner and outer border lines, following the isophotal contours. The resulting ellipses and the points used in this fit are shown in Fig. 9. The ellipticities found for the outer and inner edge are 0.991 and 0.992, respectively. Both ellipses are almost circular and concentrical. The outer ring radius is 4".5 and the inner one is 3".8. Then, a mean radius of 4".1 (16.7 h_{50}^{-1} *kpc*) can be taken for this ring. Note that, in the present case, the circular shape of the ring implies (if it is a gravitational lens) that the gradient of the gravitational potential is weak at the place of the galaxy #373 and then that the contribution of the local mass of the cluster is not dominant.

In the gravitational lens hypothesis, it is possible to determine the total mass inside the region defined by the ring by using the expression (Zwicky 1937):

$$M = \frac{c^2}{4G} \frac{D_{os}}{D_{ol} D_{ls}} R^2$$

where R is the radius of the ring and D_{ij} are the angular diameter distances between i and j. The indices o, l and s identify the observer, the lens galaxy and the source, respectively. Given the redshift of the cluster, which is 0.1756, the value of M is only a function of the source redshift. Nevertheless, M varies slowly with the redshift of the source, and it tends to an assymptotic value for high redshift sources ($z_s \geq 1.5$). Taking this assymptotic value and considering the uncertainties in R, the value of M ranges between 1.8 10^{12} h_{50}^{-1} $M_\odot$ and 2.5 10^{12} h_{50}^{-1} $M_\odot$. The lens galaxy is one of the brightest galaxies in the cluster, with B=20.24. Its absolute B magnitude is M_B=−20.46 or M_B=−20.80 according as wether we use Bruzual & Charlot's (1991) model or Rocca & Guiderdoni's (1988) model to compute the k+e corrections. The luminosity is then L_B=2.4 10^{10} h_{50}^{-2} $L_{\odot B}$ or 3.2 10^{10} h_{50}^{-2} $L_{\odot B}$ with $M_{\odot B}$=5.48. These values give respectively a global M/L_B ratio in the B filter of about 85 h_{50} or 65 h_{50} for the region, with reasonable values ranging from 75 to 100 or 60 to 80, taking all uncertainties into account. Anyhow, these values have to be considered only as an order of magnitude estimate of the local masses and M/L ratios.

4. Summary of the results and discussion

The first aim of this paper is to put together all the new photometric and spectroscopic results obtained since 1987 on the arc structures in the center of A2218. This is the first time that spectroscopic information on these arcs is available and that it is possible to discuss the nature of this phenomenon in the case of A2218. The main results obtained are the following:

1. 32 arcs and arclets have been detected in a field of about 4′× 3′ centered on the cD galaxy. Most of these arclets are not resolved perpendicular to their major axis and show an orientation which is almost perpendicular to a position vector that crosses the cD halo. In general, these objects have colour indices which are completely different from the cluster galaxies. The photometric redshifts calculated from the Bgrz photometry show that only 7 of them are compatible with the redshift of the cluster, and that most of the arcs are compatible with high redshift galaxies ($z > 0.6$).
2. We have obtained the spectra of 3 arcs in the field. Two of them clearly correspond to high redshift galaxies: #289, at z=1.034, and #359, at z=0.702. The third one is compatible with a foregound galaxy, as well as with a very high redshift galaxy, from a photometric point of view. A redshift of 0.09 is in good agreement with the photometric properties, the shape of the continuum and a possible absorption feature at 5651Å, but absolutely not with the shape of the object.
3. We report the presence of an almost complete ring around the galaxy #373 and we give a first estimation of the mass in the gravitational lens hypothesis.

From a purely observational point of view, our results confirm the importance of the seeing on the detection and photometry

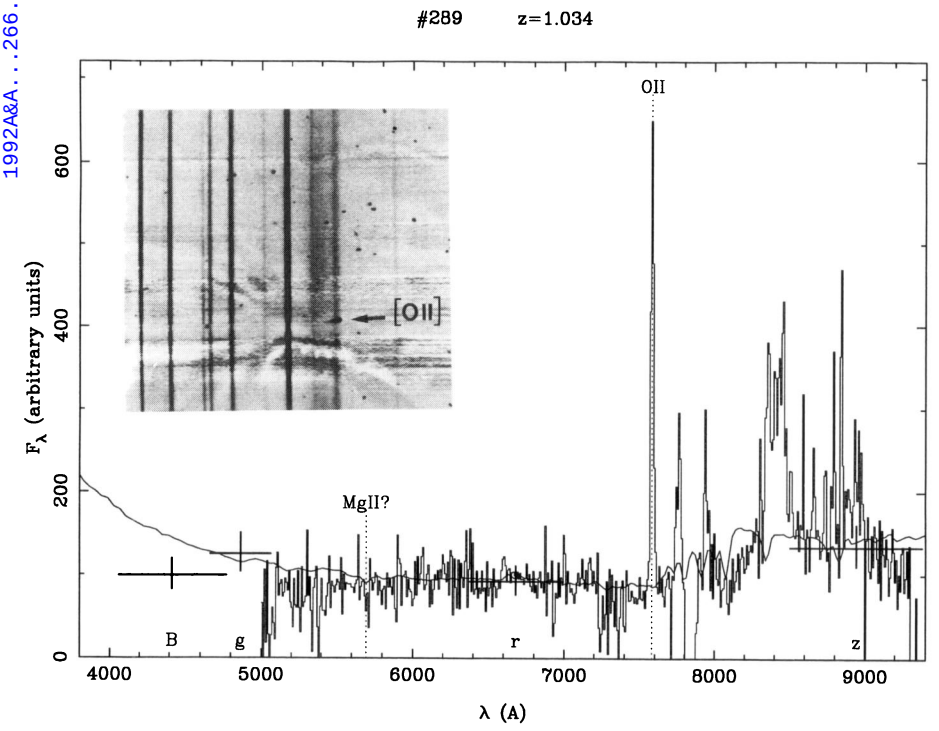

Fig. 8. Spectrum of the arc #289 showing a strong emission line at 7581Å.

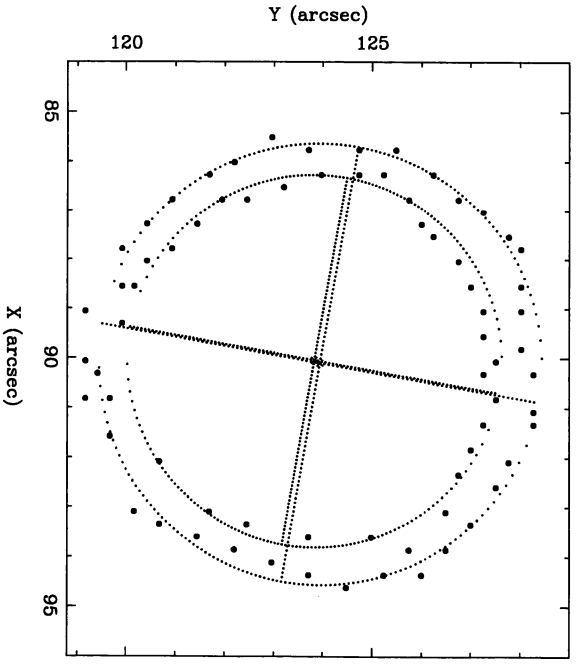

Fig. 9. Elliptical fit of the inner and outer edges of the ring around galaxy #373. The points used in this fit are also plotted. Units are in arc sec.

of such structures. It is almost impossible to detect (or even to recognize) such faint and non-resolved objects when the seeing is worst than 1″. Besides of this, the CCD acquisition method we used, which is similar to the "shift and add" proposed by Tyson (1988), produces images of improved quality with respect to the old "long -single -exposure" procedure.

From the spectroscopic results obtained, the gravitational lens hypothesis is confirmed in at least two cases. Besides of this, we justify the reliability of this assumption in the case of other arcs and arclets using only geometrical considerations, together with the photometric information in at least 4 filters. The case of object #730 is important because it is one of the "giant" non-fragmentary arc structures. The results obtained on the geometry of the whole field show that there is a potential well centered around the central cD. Nevertheless, the secondary system around galaxies #244 and #259 tend to prove that the mass distribution is more complex than a single potential well:

1. the curvature center of object #730 is located between the cD and the galaxies #244 and #259;
2. the object #289 (z=1.034) is sensibly "straight", and
3. the faint prolongation of object #289 is slightly but clearly curved, and its curvature center is located towards the opposite side with respect to the cD.

Besides of this, there are several arclets, away from the center of the cD, which show orientations compatible with a globaly elongated mass distribution. The possibility that these two systems, the cD and galaxies #244 and #259 as a whole, form a double dynamical system, is strongly supported by their radial velocities in the rest frame of the cluster (-657 km s^{-1} and +569 km s^{-1}, respectively) . The peculiar velocity of the central cD seems to indicate that we are dealing with a non-completely virialized system, with a complex dynamical structure (Malumuth 1992). The presence of two different arc systems give the first direct view of such a guess. But this is difficult to reconcile with the very extended halo of the cD galaxy.

As this cluster shows different arc structures, at different source redshifts, it is possible in principle to give an estimate of the mass distribution inside the cluster. Consider first the arc #359 (z=0.702) and the whole northern structure, with curvature centers which are located very close to the center of the cD, and position radius of 21″ (84 h_{50}^{-1} *kpc*) and 28″ (112 h_{50}^{-1} *kpc*) respectively. Assuming that these arcs are located close to the

Einstein radius of a spherical potential centered on the cD, we find a value of the total mass inside this radius between 1.4 and 2.1 10^{14} h_{50}^{-1} $M_\odot$, so a critical density ranging from 6.3 10^9 to 5.3 10^9 $M_\odot$ kpc^{-2}. When the arc #289 (z=1.034) is considered, wich is located 256 h_{50}^{-1} *kpc* away from the center of the cD, we obtain an estimate for the mass inside the volume defined by this radius of about 1.2 10^{15} h_{50}^{-1} $M_\odot$. Nevertheless, it is not possible to continue with these simple "order-of-magnitude" calculations far away from the neighbourhood of the cD galaxy without taking into account the complexity of the arc system around galaxies #244 and #259, as we already mentioned above. This global problem will need a detailed model calculation in which the possibility of a secondary potential well, or a double dynamical system is taken into account.

As a final remark, consider again the ring around the galaxy #373. The lensing hypothesis leads to a mass $\sim$2. 10^{12} h_{50}^{-1} $M_\odot$ for this galaxy, which corresponds to a M/L_B ratio $\sim$80. Such values are quite similar to those derived from the interpretation of X-ray emission of non-cD ellipticals (see e.g. Trimble 1987). The cluster mass is thus probably not dominant in this lens. The circular shape of the ring points to the same conclusion. In any case, more information is needed in order to determine the nature of this ring, before trying to use it as a serious estimator of the local mass. In particular, the spectroscopic information is crucial to confirm or to reject the gravitational lens hypothesis, and this is one of our priorities for the next future.

Acknowledgements. We are very grateful to M. Breare for his support during the observations with FOS at the WHT at La Palma, and to the technical staffs of the CAHA and Pic du Midi for their help during the different photometric runs. We acknowledge M. Cailloux, Y. Mellier, J.P. Picat and G. Soucail for their useful comments and discussions about this subject. We wish to thank Dr. G. Bruzual for allowing the use of his code for the spectral evolution of galaxies, and Dr. Gavazzi, the referee of this paper, for his comments. This work was part of the Barcelona-Toulouse ESO - keyprogram "Arc survey". It was supported by the Spanish DGICYT programs P89-0246 and PB90-0448 of the Ministerio de Educación y Ciencia, and by a grant of the "Programme Mercure" of the Spanish DGICYT of the Ministerio de Educación y Ciencia and the French Direction de la Coopération Scientifique et Technique of the Ministère des Affaires Etrangères.

References

Abell G.O, Corwin H.G. and Olowin R.P., 1989, ApJS 70, 1
Allington-Smith J.R., Breare M., Carrasco B.E., et al., 1989, MNRAS 238, 603
Birkinshaw M., Gull S.F. and Northover K.J.E., 1981, MNRAS 197, 571
Birkinshaw M. and Gull S.F., 1984, MNRAS 206, 359
Bruzual G. and Charlot S., 1991, preprint
Butcher H. and Oemler A. Jr., 1984, ApJ 285, 426
Butcher H., Oemler A. Jr. and Wells D.C., 1983, ApJS 52, 183
Fort B., 1990, in Gravitational Lensing, Lecture Notes in Physics 369, ed. Y. Mellier, B. Fort and G. Soucail, Springer Verlag, p. 221.
Fort B., 1991, Proceedings of the International Conference on Gravitational Lensing, Hamburg; eds. J. Kaiser and T. Schramm, Lecture Notes in Physics, in press.
Fort B., LeFèvre O., Hammer F. and Cailloux M., 1992, letter submitted to ApJ.
Hewitt J.N., Turner E.L., Schneider D.P., et al., 1988, Nat 333, 537
Klein U., Rephaeli Y., Schlickeiser R. and Wielebinski R., 1991, A&A 244, 43
Kristian J., Sandage A. and Westphal J.A., 1978, ApJ 221, 383
Kochanek C., Blandford, R., 1991, ApJ 375, 492
Langston G.I., Schneider D.P., Conner S., et al., 1989, AJ 97, 1283
Le Borgne J.F., Pelló R. and Sanahuja B., 1992, A&AS in press
Malumuth, E.M., 1992, ApJ 386, 420.
Partridge R.B., Perley R.A., Mandolezi N. and Delphino F., 1987, ApJ 317, 112
Pelló R. 1990, Ph. D. Thesis, University of Barcelona.
Pelló-Descayre R., Soucail G., Sanahuja B., Mathez G. and Ojero E., 1988, A&A 190, L11
Rocca-Volmerange B and Guiderdoni B., 1988, A&AS 75, 93
Trimble V., 1987, ARA&A 25, 425
Tyson J.A., 1988 AJ 96, 1
Visvanathan N. and Sandage A., 1977, ApJ 216, 214
Zwicky F., 1937, Phys. Rev. Lett. 51, 679

This article was processed by the author using Springer-Verlag TEX A&A macro package 1991.